HHS Public Access

Author manuscript

JACC Cardiovasc Interv. Author manuscript; available in PMC 2017 January 12.

Published in final edited form as:

JACC Cardiovasc Interv. 2016 May 09; 9(9): 959–970. doi:10.1016/j.jcin.2016.01.032.

Magnetic Resonance Imaging–Guided Transcatheter Cavopulmonary Shunt

Kanishka Ratnayaka, MD[a,b], **Toby Rogers, BM, BCh**[a], **William H. Schenke, BS**[a], **Jonathan R. Mazal, MS**[a], **Marcus Y. Chen, MD**[a], **Merdim Sonmez, PhD**[a], **Michael S. Hansen, PhD**[a], **Ozgur Kocaturk, PhD**[a], **Anthony Z. Faranesh, PhD**[a], and **Robert J. Lederman, MD**[a]

[a]Cardiovascular and Pulmonary Branch, Division of Intramural Research, National Heart, Lung, and Blood Institute, Bethesda, Maryland [b]Division of Cardiology, Children's National Medical Center, Washington, District of Columbia

Abstract

OBJECTIVES—The aim of this study was to test the hypothesis that real-time magnetic resonance imaging (MRI) would enable closed-chest percutaneous cavopulmonary anastomosis and shunt by facilitating needle guidance along a curvilinear trajectory, around critical structures, and between a superior vena cava "donor" vessel and a pulmonary artery "target."

BACKGROUND—Children with single-ventricle physiology require multiple open heart operations for palliation, including sternotomies and cardiopulmonary bypass. The reduced morbidity of a catheter-based approach would be attractive.

METHODS—Fifteen naive swine underwent transcatheter cavopulmonary anastomosis and shunt creation under 1.5-T MRI guidance. An MRI antenna-needle was advanced from the superior vena cava into the target pulmonary artery bifurcation using real-time MRI guidance. In 10 animals, balloon-expanded off-the-shelf endografts secured a proximal end-to-end caval anastomosis and a distal end-to-side pulmonary anastomosis that preserved blood flow to both branch pulmonary arteries. In 5 animals, this was achieved with a novel, purpose-built, self-expanding device.

RESULTS—Real-time MRI needle access of target vessels (pulmonary artery), endograft delivery, and superior vena cava shunt to pulmonary arteries were successful in all animals. All survived the procedure without complications. Intraprocedural real-time MRI, post-procedural MRI, x-ray angiography, computed tomography, and necropsy showed patent shunts with bidirectional pulmonary artery blood flow.

CONCLUSIONS—MRI guidance enabled a complex, closed-chest, beating-heart, pediatric, transcatheter structural heart procedure. In this study, MRI guided trajectory planning and reproducible, reliable bidirectional cavopulmonary shunt creation.

REPRINT REQUESTS AND CORRESPONDENCE: Dr. Robert J. Lederman, Cardiovascular and Pulmonary Branch, Division of Intramural Research, National Heart, Lung, and Blood Institute, National Institutes of Health, Building 10, Room 2c713, MSC 1538, Bethesda, Maryland 20892-1538. lederman@nih.gov.

The authors have reported that they have no relationships relevant to the contents of this paper to disclose.

APPENDIX For a supplemental video and its legend, please see the online version of this article.

Keywords

congenital heart disease; image-guided intervention; interventional MRI; real-time MRI; sutureless anastomosis; vascular shunt

Children born with single-ventricle physiology require several cardiac surgical procedures in order to survive. Surgical management requires multiple sternotomies and cardiopulmonary bypass runs. A transcatheter alternative would be attractive to reduce procedural morbidity.

Traditional single-ventricle procedures shunt, or divert, blood flow to sustain systemic or pulmonary circulation. A first-stage systemic–to–pulmonary artery shunt may be needed in a newborn. The second stage is the Glenn shunt, which redirects superior vena cava blood to the pulmonary arteries (1,2). The third or Fontan stage redirects inferior vena cava blood to the pulmonary arteries.

Enhanced imaging guidance, available in real time, might allow nonsurgical percutaneous catheter creation of similar shunts. Real-time magnetic resonance imaging (MRI) provides enhanced procedure guidance compared with radiography in that it offers continuous soft tissue and blood visualization and compared with ultrasound in that it can be viewed in any orientation with a large field of view (FOV).

We hypothesized that MRI guidance alone would enable needle navigation along a nonlinear trajectory, around critical structures, and between noncontiguous vessels to create a percutaneous cavopulmonary shunt that preserves blood flow to both branch pulmonary arteries. We tested the safety and feasibility of this minimally invasive approach in healthy animals.

METHODS

ANIMAL PROCEDURES

Animal procedures were approved by the Institutional Animal Care and Use Committee and followed contemporary National Institutes of Health guidelines. Fifteen naive York-shire swine were anesthetized and mechanically ventilated. Percutaneous arterial, venous, and pericardial access was obtained. Hemodynamic recordings, selective contrast angiography (radiography), and diagnostic MRI were performed before and after intervention. Heparin maintained activated clotting times >250 s.

MRI

Experiments were conducted in a combined interventional cardiovascular MRI and radiographic fluoroscopy suite (1.5-T Aera and Artis Zee, Siemens Healthcare, Erlangen, Germany).

Segmented MRI used the following typical parameters. For steady-state free precession (SSFP), repetition time (TR) 2.7 ms, echo time (TE) 1.2 ms, flip angle 66°, bandwidth 930 Hz/pixel, FOV 340 × 276 mm, matrix size 192 × 156 pixels, slice thickness 6 mm. For velocity-encoded gradient echo, TR 4.6 ms, TE 2.5 ms, flip angle 20°, bandwidth 449 Hz/

pixel, FOV 340 × 287 mm, matrix size 192 × 146 pixels, slice thickness 6 mm, velocity encoding 100 to 200 cm/s, 1 signal average. For time-resolved angiography with stochastic trajectories, TR 2.7 ms, TE 0.99 ms, flip angle 30°, bandwidth 630 Hz/pixel, FOV 300 × 300 × 114, matrix 320 × 224 × 88, voxel size 0.9 × 0.9 × 1.3, generalized autocalibrating partially parallel acquisitions (GRAPPA) factor 8, 30 measurements, temporal resolution 1.16 s. For 3-dimensional radial SSFP of the whole heart, TR 3.1 ms, TE 1.56 ms, flip angle 115°, bandwidth, 898 Hz/pixel, FOV 220 × 220 mm, voxel size 1.1 × 1.1 × 1.1 mm, base resolution 192, 12,360 radial views.

Real-time MRI for interventional procedures used SSFP (TR 2.8 ms, TE 1.4 ms, flip angle 45°, bandwidth 1,000 Hz/pixel, matrix size 192 × 144, FOV 300 × 300 mm, GRAPPA factor 2) or gradient echo (TR 4.2 ms, TE 1.9 ms, flip angle 15°, bandwidth 500 Hz/pixel, matrix size 192 × 144, FOV 300 × 300 mm, GRAPPA factor 2 to 4 interactively to achieve 5 to 10 frames/s), and interactive saturation pre-pulses to enhance the visibility of gadolinium-filled balloons.

REAL-TIME MRI-GUIDED TRAJECTORY PLANNING

Real-time MRI guided all procedural steps (Figure 1). First we planned a curvilinear trajectory to avoid aortic puncture, to preserve right upper pulmonary artery flow, to attain precise entry at the junction of the main pulmonary artery and right pulmonary artery, and to achieve in-line access to the left pulmonary artery for optimal guidewire placement (Figure 2). Then we advanced a custom MRI antenna-needle (3) along this trajectory toward the target pulmonary artery bifurcation. Next, the pulmonary artery was entered, and position was confirmed by injecting 1% gadopentetate (Magnevist, Bayer, Whippany, New Jersey) through the needle (Figure 3).

REAL-TIME MRI-GUIDED ANASTOMOSIS AND SHUNT CREATION

Over a nitinol guidewire, we exchanged the needle for a vascular introducer sheath, customized with iron-oxide paint (iron oxide 5 microns [Sigma-Aldrich, St. Louis, Missouri] in low-viscosity, silicone dispersion [MED 6400, NuSil, Carpinteria, California] heat-cured overnight) to make the sheath tip and dilator tip visible on MRI.

OFF-THE-SHELF ENDOGRAFTS

Because available commercial endografts were too short, sequential overlapping pre-mounted covered CP Stents (12 to 18 mm in diameter, 45 mm in length; NuMed, Hopkinton, New York) were delivered and expanded using balloons (1 to 2 mm oversized) filled with 1% gadopentetate (Figure 4).

NOVEL PURPOSE-BUILT CAVOPULMONARY ANASTOMOSIS AND SHUNT DEVICE

We designed a custom endograft (Figure 5) with the following performance requirements:

- Hemostatic proximal end-to-end anastomosis (superior vena cava)
- Hemostatic distal end-to-side anastomosis (pulmonary artery)

- Divert superior vena cava blood flow from right atrium to both branch pulmonary arteries
- MRI safe and visible (easy to distinguish from [without obscuring] background anatomy)
- Hemocompatibility and biocompatibility
- Occlude the azygous vein

An accompanying delivery system had the following requirements:

- Ability to hold, reposition, deploy, and retrieve the device before final release
- Guidewire compatible with injection port
- MRI safe and visible

The devices (Transmural Systems, Andover, Massachusetts) were deployed in the final 5 animals (Figure 6, Online Video 1). The devices were 12 to 14 mm in diameter and 75 mm in length, with a 3- to 5-mm intrapulmonary retention disk diameter.

FOLLOW-UP MEASUREMENTS AND DATA ANALYSIS

Animals were observed for 6 h after the procedure to detect complications. Follow-up hemodynamic status, x-ray angiography, MRI, and 320–detector row computed tomography (CT) (Aquilion ONE, Toshiba, Tokyo, Japan) were performed.

We recorded success or failure of needle access and anastomosis, number of needle attempts, complications, and procedure duration. Shunts were measured using both the Fick method and velocity-encoded MRI. Differential pulmonary artery branch flow was evaluated by velocity-encoded MRI. Blood was tested using bedside human assays for chemistry (i-Stat, Abbott, Princeton, New Jersey), oximetry (Avox, San Antonio, Texas), and coagulation (Hemachron, ITC, Edison, New Jersey).

Results are expressed as mean ± SD. Pre- and post-intervention data were analyzed using 2-tailed paired Student *t* tests (Excel 2010, Microsoft Corporation, Redmond, Washington); p values <0.05 were considered significant.

RESULTS

Fifteen naive juvenile animals (mean weight 22.5 ± 3.4 kg) were studied. MRI guided all procedures. Oblique coronal, sagittal, and axial real-time MRI planes were used to guide curvilinear trajectories and to facilitate anastomosis and shunt creation (Figures 2, 4, and 6).

REAL-TIME MRI-GUIDED TRAJECTORY PLANNING

Real-time MRI-guided needle access was successful in all animals (Figure 3). All were accomplished on the first needle puncture attempt. Intraprocedural real-time MRI, post-intervention MRI, x-ray angiography, CT, and necropsy showed that aortic injury was avoided, right upper pulmonary artery blood flow was preserved, and main pulmonary

artery–right pulmonary artery junction entry was attained. In all animals, real-time MRI-guided trajectory planning enabled in-line needle access to left pulmonary artery for optimal guidewire placement.

REAL-TIME MRI-GUIDED ANASTOMOSIS AND SHUNT CREATION

Real-time MRI-guided endograft delivery and superior vena cava–to–pulmonary artery shunt steps were successful in all animals (Figures 4 and 6 to 8, Online Video 1). Intraprocedural real-time MRI, post-intervention MRI, x-ray angiography, CT, and necropsy showed appropriately positioned endografts, patent cavopulmonary shunts, and bidirectional pulmonary blood flow distribution (Figures 7 and 8). Superior vena cava blood flow was diverted from the right atrium into the pulmonary arteries as planned, and the azygos vein was intentionally excluded as in conventional surgical Glenn shunts. The distal endograft edge encroached on the right pulmonary artery lumen but permitted blood flow, including to the right upper pulmonary artery.

As expected, there was no significant intracardiac shunt or change in Qp/Qs (by oximetry or by velocity-encoded MRI). Right ventricular volumes tended to decrease but not with statistical significance. Superior vena cava and left pulmonary artery dimensions did not change. Superior vena cava blood pressure increased as expected (Tables 1 and 2). There was no superior vena cava–to–pulmonary anastomosis peak systolic pressure gradient. A 3.7 ± 2.9 mm Hg peak systolic pressure gradient to the right pulmonary artery was present.

PROCEDURAL DETAILS AND COMPLICATIONS

Total procedure time was 78:09 ± 22:59 min, including trajectory planning (1:43 ± 1:16 min), active needle access (5:13 ± 2:07 min), and endograft delivery (31:52 ± 18:50 min). Commercial endograft delivery time (42:05 ± 15:26 min) was significantly longer than for the novel, purpose-built device (13:28 ± 4:10 min; $p = 0.001$).

Pericardial blood that accumulated during sheath exchange (64.1 ± 77 ml) was immediately reinfused, analogous to intraoperative autotransfusion. In 7 of 15 animals, there was no pericardial blood accumulation. Net blood loss was minimal (baseline hemoglobin 7.6 ± 0.8 g/dl, post-procedure 8.2 ± 1 g/dl; $p = 0.13$). No animals experienced hemothorax or pneumothorax, hemopericardium or pneumopericardium, sustained dysrhythmia, or death. Necropsy demonstrated no nearby hematoma or mural disruption, including at the pulmonary artery anastomosis (Figure 8). Mean activated clotting time was 389 ± 160 s.

DISCUSSION

We describe the key cavopulmonary anastomosis step for an eventual wholly percutaneous transcatheter Glenn procedure as an alternative to surgery requiring median sternotomy and cardiopulmonary bypass. This is the first description of a percutaneous cavopulmonary shunt achieving pulmonary blood flow to both pulmonary artery branches (“bidirectional Glenn”). This solely MRI approach offers continuous visualization of superior vena cava “donor” vessel and pulmonary artery “target” vessel; therefore, it does not require pre-positioning of a catheter or snare in the target pulmonary artery, a procedural step that may not always be easily accomplished in small children with single-ventricle physiology. We also describe

early pre-clinical evaluation of a novel purpose-built cavopulmonary shunt device. This work anticipates future MRI-guided, wholly percutaneous Fontan completion using a purpose-built inferior cavopulmonary connection device.

Clinical experience with MRI catheterization and MRI electrophysiology continues to accrue (4–6), including simple cardiac intervention (7). Interventional cardiac MRI may enable or enhance novel percutaneous structural heart and congenital heart disease interventional procedures (8–10). In this feasibility study, MRI enabled a surgical alternative using percutaneous techniques because of excellent soft tissue visualization in any imaging plane. Real-time MRI guided needle access of noncontiguous vessels and allowed the creation of both end-to-end caval and end-to-side pulmonary anastomoses in all animals, along with intentional exclusion of the azygos vein.

Stand-alone MRI guidance was critical to the success of this procedure. First, curvilinear trajectory planning enabled transmural needle puncture across 1 vessel wall (superior vena cava) into a neighboring target vessel (pulmonary artery). Second, real-time MRI enabled the operator to deflect a straight needle through extravascular space around critical structures (aorta, right upper pulmonary artery), precisely entering the main pulmonary artery–right pulmonary junction with in-line access to the left pulmonary artery for optimal guidewire placement. Third, MRI provided continuous real-time depiction of the distal target (without repeated contrast injections) to create an end-to-side anastomosis that preserved bidirectional pulmonary blood flow. Interactive imaging specifically averted injury to critical surrounding structures. MRI allowed us to adjust needle trajectory and selected MRI planes (views) interactively in real time to correct displacement of imaging targets caused by cardiac motion, respiratory motion, and rigid catheter instruments. Although theoretically feasible, these adjustments would have been difficult using roadmaps, such as angiography or coregistered cone-beam or prior CT, because the fused roadmaps easily become outdated and misleading when tissues are distorted by catheter devices. We also found it useful to adjust temporal resolution (“speeding up the MRI”) during specific technically demanding steps, such as needle access to the pulmonary artery and endograft deployment.

Our work builds on the work of others. In animals, x-ray guided aortopulmonary shunts have been created using docking magnets or radiofrequency perforation followed by stent implantation (11,12). In patients, percutaneous palliative Potts (left pulmonary artery–to–descending aorta) shunts have been achieved in adults with end-stage pulmonary artery hypertension, using x-ray guided wire puncture into pre-positioned snare targets followed by endografts (13). Clinical vessel-to-atria “fenestrations” have been created using x-ray guided transseptal needle puncture and endografts (14). Two previous reports achieved x-ray guided percutaneous right-sided, unidirectional “classic” Glenn shunts that did not preserve bidirectional pulmonary blood flow. Levi et al. (11) used x-ray transseptal needle puncture (from the superior vena cava) aimed at prepositioned pulmonary artery angioplasty balloon “targets” to establish right-sided unidirectional Glenn circulation in 2 animals. Similarly, Schmitt et al. (15) used radiofrequency energy to traverse tissue into balloon catheter targets pre-positioned in the right pulmonary artery and establish right-sided, unidirectional Glenn shunts. Although snare or balloon targets are easily positioned into the pulmonary artery in normal anatomy, for clinical translation, such targets would have to be delivered through

small shunts (Blalock-Taussig or Sano) or pulmonary artery obstructions (subvalvular/valvular/supravalvular stenosis or surgical pulmonary artery bands). In practice, these maneuvers are possible, but pose technical challenges, and may cause significant hemodynamic compromise such as hypotension or cyanosis.

By contrast, our work achieved cavopulmonary anastomosis and shunt similar to the contemporary surgical bidirectional Glenn procedure (2) guided by stand-alone real-time MRI. Continuous anatomic imaging with excellent soft tissue visualization obviated the need for a pre-positioned distal target balloon, snare, or catheter. Imaging allowed us to select a specific anastomotic target and to avoid catastrophic target miss. We selected the junction of the main and right pulmonary arteries, in line with the left pulmonary artery, so that the endograft would redistribute flow to both pulmonary artery branches. “Classic” unidirectional Glenn shunts, which have distal end-to-end anastomoses, are less technically demanding.

We were first able to accomplish a transcatheter bidirectional cavopulmonary shunt using commercially available endografts that provided a suboptimal distal anastomosis. We therefore designed and tested a novel, purpose-built cavopulmonary anastomosis and shunt device. This custom endograft simplified the procedure and allowed implantation in one-quarter of the procedure time. Compared with off-the-shelf tube endografts, the custom flared endograft had superior deliverability, usability, and MRI visibility and a potentially more secure distal anastomosis. The flanged anastomosis device helped operators avoid catastrophic target miss.

By design, our percutaneous superior cavopulmonary shunt strategy does not interfere with the caudal pulmonary artery, in order to allow later completion of the Fontan using surgical or transcatheter techniques.

STUDY LIMITATIONS

Wholly MRI-guided procedures, as described here, are limited by commercial availability of MRI-visible and MRI-safe catheter devices. Device modification will be required to translate this work into patients. Our laboratory is developing the “active” MRI needle for human use (3); passive MRI needles, though less conspicuous, are commercially available today. Similarly, our laboratory is developing a family of MRI-safe, exchange-length guidewires, both active and passive, and iron oxide–tipped introducer sheaths for MRI visibility. Commercially available endografts and the novel, purpose-built, cavopulmonary anastomosis and shunt device are MRI visible and safe. There is no ideal animal model to mimic the cavopulmonary anatomic relationship and human single-ventricle physiology (16). Animals in this study were larger than contemporary Glenn surgical patients, but similar techniques and devices can be used in small children. Conversion to passive pulmonary blood flow physiology resulted in decreased ventricular ejection fraction and cardiac output in naive animals (Table 2). Differential pulmonary artery branch flow may have been better assessed by flow wires (vs. velocity-encoded MRI), because metal artifact likely affected post-intervention measurement. Nevertheless, right pulmonary artery dimensions were smaller and could have been improved by post-intervention right

pulmonary artery balloon angioplasty (which was not attempted). This could have also improved vessel (right pulmonary artery) apposition of the novel device.

CONCLUSIONS

Using MRI for its superior soft-tissue visualization enabled a completely catheter-based extra-anatomic bypass for congenital heart disease and averted open surgical exposure and cardiopulmonary bypass. This created a cavopulmonary shunt with bidirectional pulmonary blood flow. Clinical translation will require specific MRI-safe device commercialization.

Supplementary Material

Refer to Web version on PubMed Central for supplementary material.

Acknowledgments

This work was supported by the Division of Intramural Research, National Heart, Lung, and Blood Institute, National Institutes of Health (grants Z01-HL005062 and Z01-HL006041 to Dr. Lederman). The National Institutes of Health and Children's National Medical Center have collaborative research and development agreements for interventional cardiovascular magnetic resonance imaging with Siemens Medical Systems. NUMED, Inc., supplied mounted covered CP Stents. Transmural Systems supplied purpose-built cavopulmonary anastomosis devices.

The authors thank Joni Taylor and Katherine Lucas of the National Heart, Lung, and Blood Institute's Animal Surgery and Resources Core for technical assistance, and Alan Hoofring of NIH Medical Arts for drawings.

ABBREVIATIONS AND ACRONYMS

CT	computed tomography
FOV	field of view
GRAPPA	generalized autocalibrating partially parallel acquisitions
MRI	magnetic resonance imaging
SSFP	steady-state free precession
TE	echo time
TR	repetition time

References

1. Glenn WW. Circulatory bypass of the right side of the heart. IV. Shunt between superior vena cava and distal right pulmonary artery; report of clinical application. N Engl J Med. 1958; 259:117–20. [PubMed: 13566431]
2. Hopkins RA, Armstrong BE, Serwer GA, Peterson RJ, Oldham HN Jr. Physiological rationale for a bidirectional cavopulmonary shunt. A versatile complement to the Fontan principle. J Thorac Cardiovasc Surg. 1985; 90:391–8. [PubMed: 4033175]
3. Saikus CE, Ratnayaka K, Barbash IM, et al. MRI-guided vascular access with an active visualization needle. J Magn Reson Imaging. 2011; 34:1159–66. [PubMed: 22006552]
4. Ratnayaka K, Faranesh AZ, Hansen MS, et al. Real-time MRI-guided right heart catheterization in adults using passive catheters. Eur Heart J. 2013; 34:380–9. [PubMed: 22855740]

5. Pandya B, Quail MA, Steeden JA, et al. Real-time magnetic resonance assessment of septal curvature accurately tracks acute hemodynamic changes in pediatric pulmonary hypertension. Circ Cardiovasc Imaging. 2014; 7:706–13. [PubMed: 24771555]
6. Sommer P, Grothoff M, Eitel C, et al. Feasibility of real-time magnetic resonance imaging-guided electrophysiology studies in humans. Europace. 2013; 15:101–8. [PubMed: 22849974]
7. Krueger JJ, Ewert P, Yilmaz S, et al. Magnetic resonance imaging-guided balloon angioplasty of coarctation of the aorta: a pilot study. Circulation. 2006; 113:1093–100. [PubMed: 16490822]
8. Raval AN, Telep JD, Guttman MA, et al. Real-time magnetic resonance imaging-guided stenting of aortic coarctation with commercially available catheter devices in swine. Circulation. 2005; 112:699–706. [PubMed: 16043639]
9. Kahlert P, Eggebrecht H, Plicht B, et al. Towards real-time cardiovascular magnetic resonance-guided transarterial aortic valve implantation: in vitro evaluation and modification of existing devices. J Cardiovasc Magn Reson. 2010; 12:58. [PubMed: 20942968]
10. Ratnayaka K, Saikus CE, Faranesh AZ, et al. Closed-chest transthoracic magnetic resonance imaging-guided ventricular septal defect closure in swine. J Am Coll Cardiol Intv. 2011; 4:1326–34.
11. Levi DS, Danon S, Gordon B, et al. Creation of transcatheter aortopulmonary and cavopulmonary shunts using magnetic catheters: feasibility study in swine. Pediatr Cardiol. 2009; 30:397–403. [PubMed: 19365662]
12. Sabi TM, Schmitt B, Sigler M, et al. Transcatheter creation of an aortopulmonary shunt in an animal model. Catheter Cardiovasc Interv. 2010; 75:563–9. [PubMed: 20066726]
13. Esch JJ, Shah PB, Cockrill BA, et al. Transcatheter Potts shunt creation in patients with severe pulmonary arterial hypertension: initial clinical experience. J Heart Lung Transplant. 2013; 32:381–7. [PubMed: 23415728]
14. Mehta C, Jones T, De Giovanni JV. Percutaneous transcatheter communication between the pulmonary artery and atrium following an extra-cardiac Fontan: an alternative approach to fenestration avoiding conduit perforation. Catheter Cardiovasc Interv. 2008; 71:936–9. [PubMed: 18412269]
15. Schmitt B, Sabi TM, Sigler M, Berger F, Ewert P. Upper cavopulmonary anastomosis by transcatheter technique. Catheter Cardiovasc Interv. 2012; 80:93–9. [PubMed: 22419619]
16. Sizarov A, de Bakker BS, Klein K, Ohlerth S. Building foundations for transcatheter intervascular anastomoses: 3D anatomy of the great vessels in large experimental animals. Interact Cardiovasc Thorac Surg. 2014; 19:543–51. [PubMed: 24994699]

PERSPECTIVES

WHAT IS KNOWN?

Real-time MRI can visualize soft tissue continuously.

WHAT IS NEW?

Real-time MRI enables percutaneous navigation of catheters outside vascular spaces to create an extra-anatomic connection between separate blood vessels, an approach that in the past has required open surgery.

WHAT IS NEXT?

In addition to the cavopulmonary shunt created in this study, other extra-anatomic bypass procedures may be possible using real-time MRI guidance and similar catheter tools. Simple modifications of commercially available catheter devices will make them safe for use under real-time MRI guidance in patients.

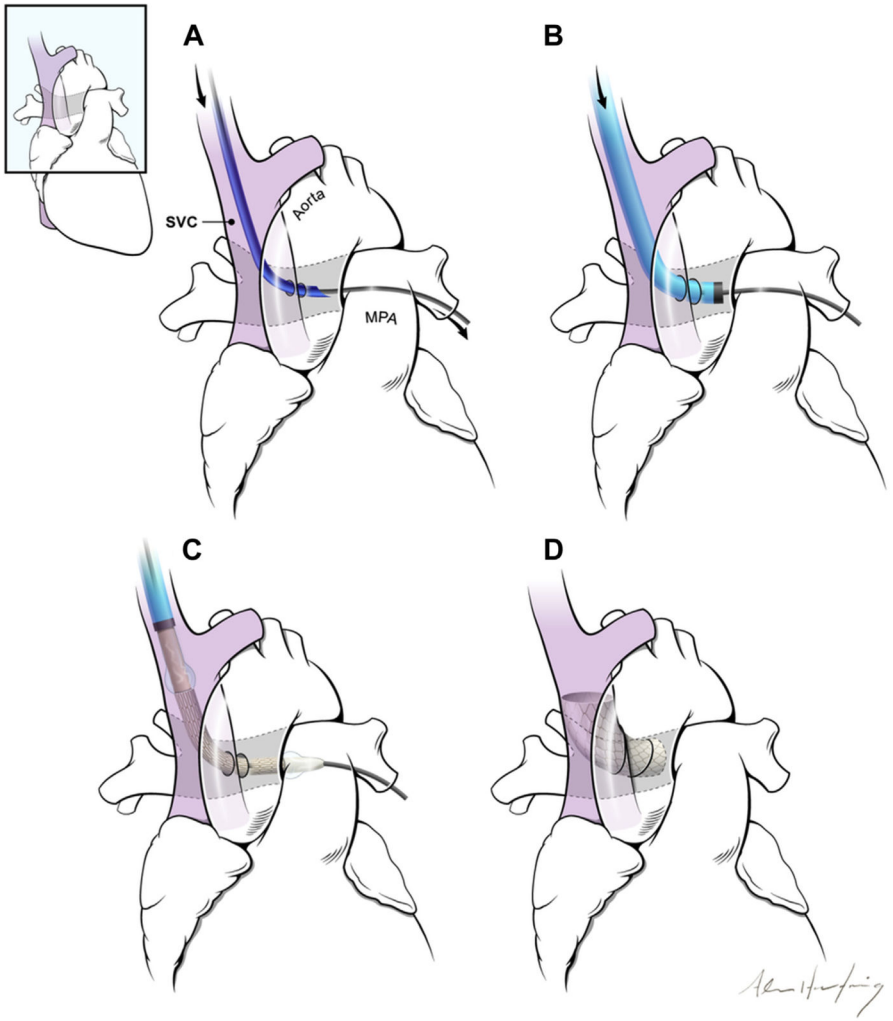

FIGURE 1. The Concept of a Percutaneous Bidirectional Cavopulmonary Shunt

(A) First, a needle **(dark blue)** is advanced from the superior vena cava (SVC) **(purple)** into the main pulmonary artery (MPA) using magnetic resonance imaging guidance. **(B)** Next, the needle is exchanged for a long introducer sheath **(light blue, black tip). (C)** The shunt is created using endografts. **(D)** The endografts divert SVC blood away from the right atrium into the pulmonary arteries, while excluding the azygos vein (not shown).

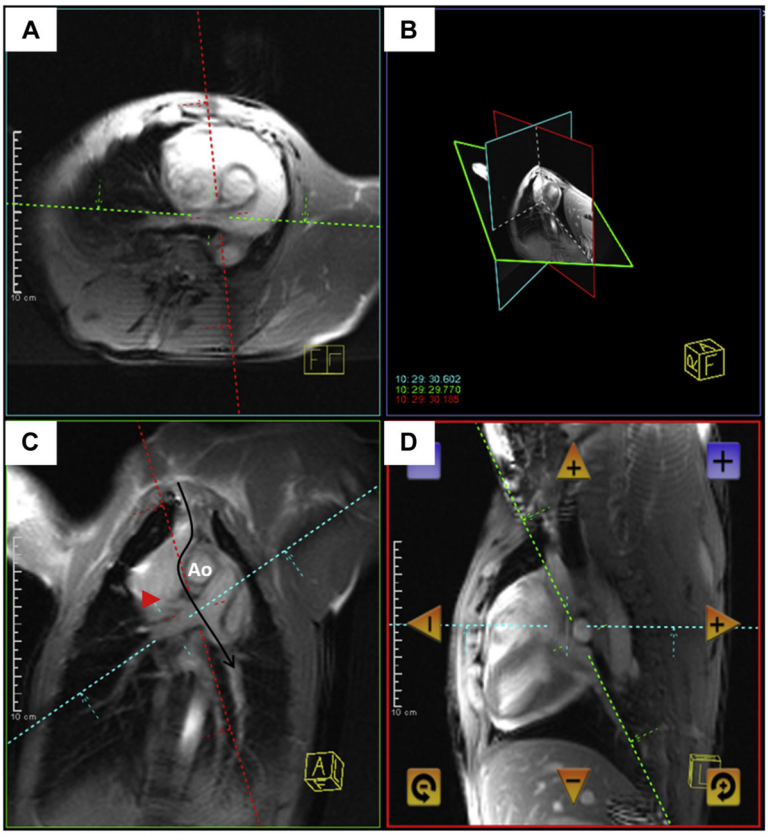

FIGURE 2. Real-Time Magnetic Resonance Imaging Needle Trajectory Planning

Magnetic resonance imaging shows a typical curvilinear **(C**, **black arrow)** trajectory plan including oblique axial **(A)**, coronal **(C)**, sagittal **(D)**, and 3-dimensional **(B)** representation of the planes, which are selected to intersect at the target pulmonary artery bifurcation. Continuous real-time imaging assists the operator in avoiding the right upper pulmonary artery branch **(red arrowhead)** and the aorta (Ao).

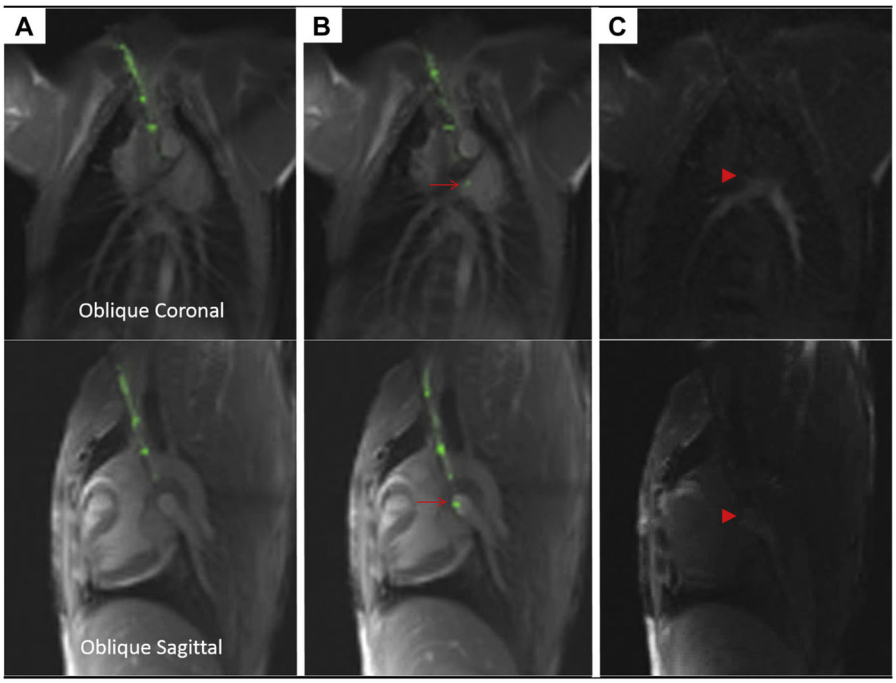

FIGURE 3. Puncturing the Pulmonary Artery Using a Magnetic Resonance Imaging Needle

This sequence depicts advancement of the magnetic resonance imaging (MRI) needle in 2 simultaneous planes, **top and bottom**. The MRI needle is advanced from the superior vena cava **(A)** and then enters the main pulmonary artery **(B)**, where the tip is indicated with a **red arrow. (C)** Gadolinium contrast is injected through the needle to confirm its intraluminal position **(red arrowhead)**.

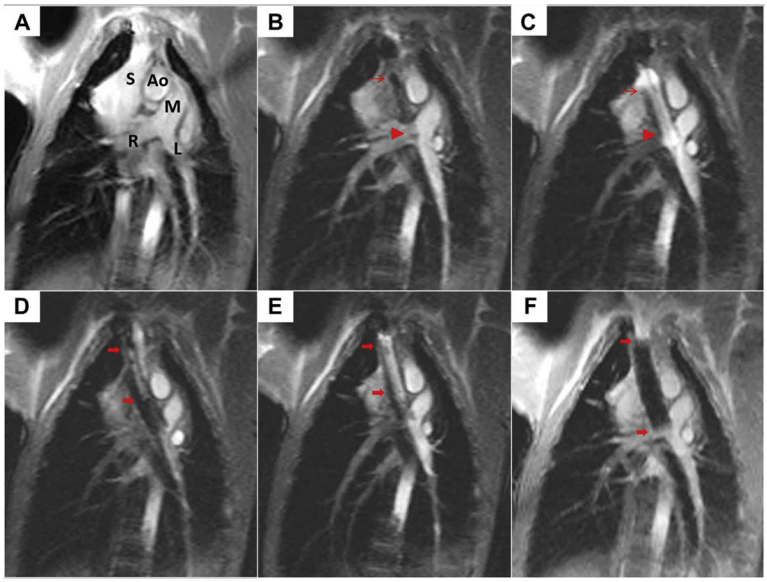

FIGURE 4. Creating the Cavopulmonary Shunt Using Real-Time Magnetic Resonance Imaging

(A) This oblique coronal working view is shown. Ao = aorta; L = left pulmonary artery; M = main pulmonary artery; R = right pulmonary artery; S = superior vena cava. **(B)** The first of 2 endografts is positioned across the wall of the pulmonary artery (**thin red arrow**, proximal endograft; **red arrowhead**, distal endograft) to allow bidirectional pulmonary blood flow. **(C)** The first endograft is expanded using a balloon filled with gadolinium contrast. **(D)** The second overlapping endograft, used for want of a longer single device, is positioned to anchor cavopulmonary conduit in the superior vena cava and exclude the azygos vein (**thick red arrows**, proximal, distal endograft). **(E)** The second endograft is deployed. **(F)** Afterward, the completed percutaneous bidirectional cavopulmonary shunt is visible using real-time magnetic resonance imaging, where it appears black.

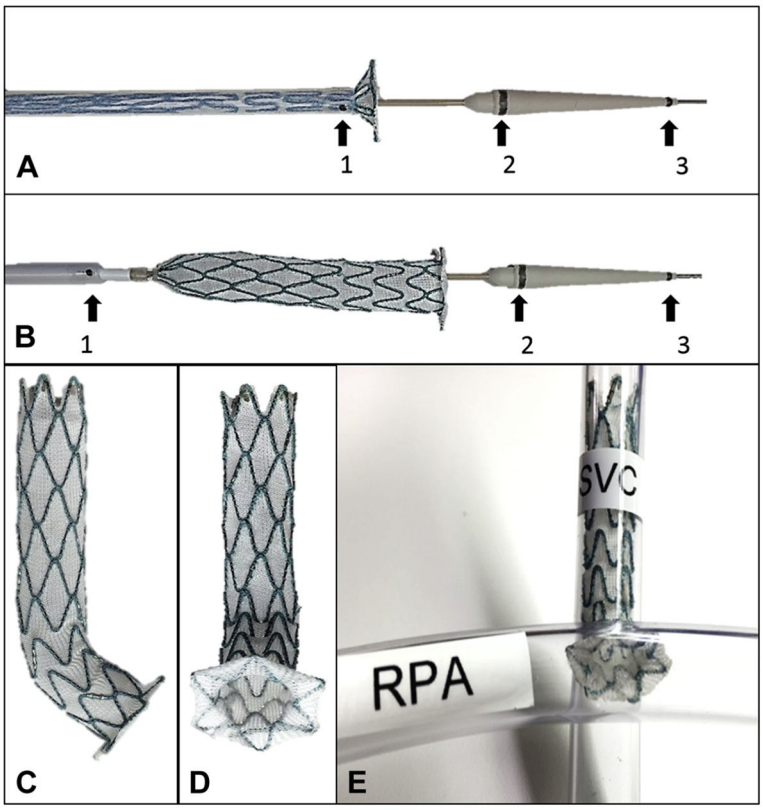

FIGURE 5. Novel Purpose-Built Cavopulmonary Shunt Device

A novel purpose-built, self-expanding cavopulmonary anastomosis device **(A to E)** and delivery **(A, B)** system (Transmural Systems, Andover, Massachusetts) was engineered to provide proximal end to end anastomosis (superior vena cava [SVC]) and distal end to side anastomosis (pulmonary artery) to divert superior vena cava blood flow from right atrium to both branch pulmonary arteries **(E)**. Magnetic resonance imaging conspicuity of delivery systems was optimized with iron oxide bands **(black arrows)** at distal sheath tip (1), proximal nose cone (2), and distal nose cone (3). RPA = right pulmonary artery.

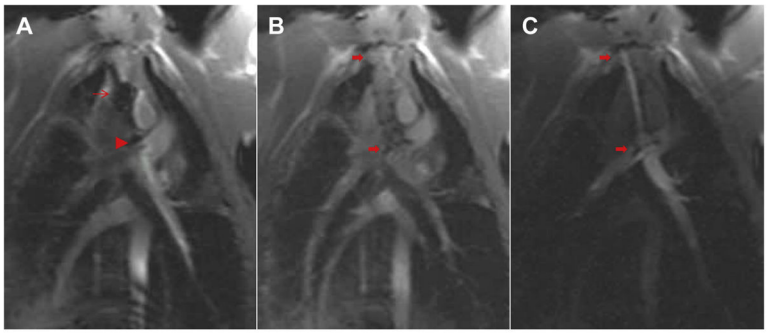

FIGURE 6. Novel Purpose-Built Cavopulmonary Shunt Procedure

An oblique coronal working view is used to advance the custom delivery system to target anatomy under real-time magnetic resonance imaging (MRI) guidance **(A)**. Delivery system iron oxide marker bands are clearly seen on MRI (**red arrow**, distal sheath tip adjoining proximal nose cone [corresponds to 1 and 2 in Figures 5A and 5B]; **red arrowhead**, distal nose cone [corresponds to 3 in Figures 5A and 5B]). After precise positioning using continuous real-time MRI visualization, the novel purpose-built, self-expanding cavopulmonary anastomosis device (**red arrows** show proximal and distal ends of the device) is deployed **(B)**. Gadolinium contrast injection into the superior vena cava with flow through the cavopulmonary anastomosis device into both branch pulmonary arteries confirms ideal placement **(C)** (Online Video 1).

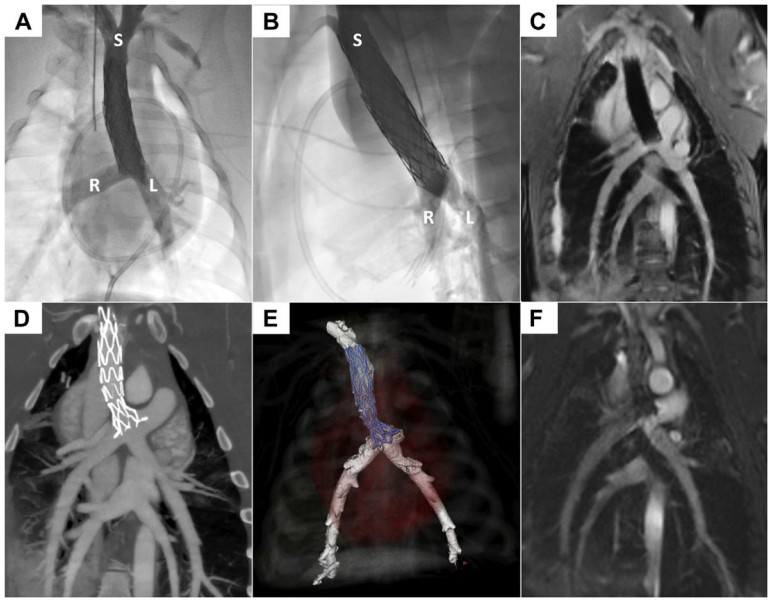

FIGURE 7. The Cavopulmonary Shunt Depicted Using Radiography, Magnetic Resonance Imaging, and Computed Tomographic Angiography

X-ray contrast angiograms are shown in straight anterior-posterior **(A)** and straight lateral **(B)** projections. L = left pulmonary artery; R = right pulmonary artery; S = superior vena cava. The 3-dimensional radial steady-state free precession whole-heart magnetic resonance image **(C)** shows the endografts (sequential, overlapping) post-deployment. Commercial endografts are shown in **A** to **C**. Computed tomography **(D, E)** and steady-state free precession magnetic resonance imaging **(F)** show the purpose-built, self-expanding cavopulmonary anastomosis device post-deployment.

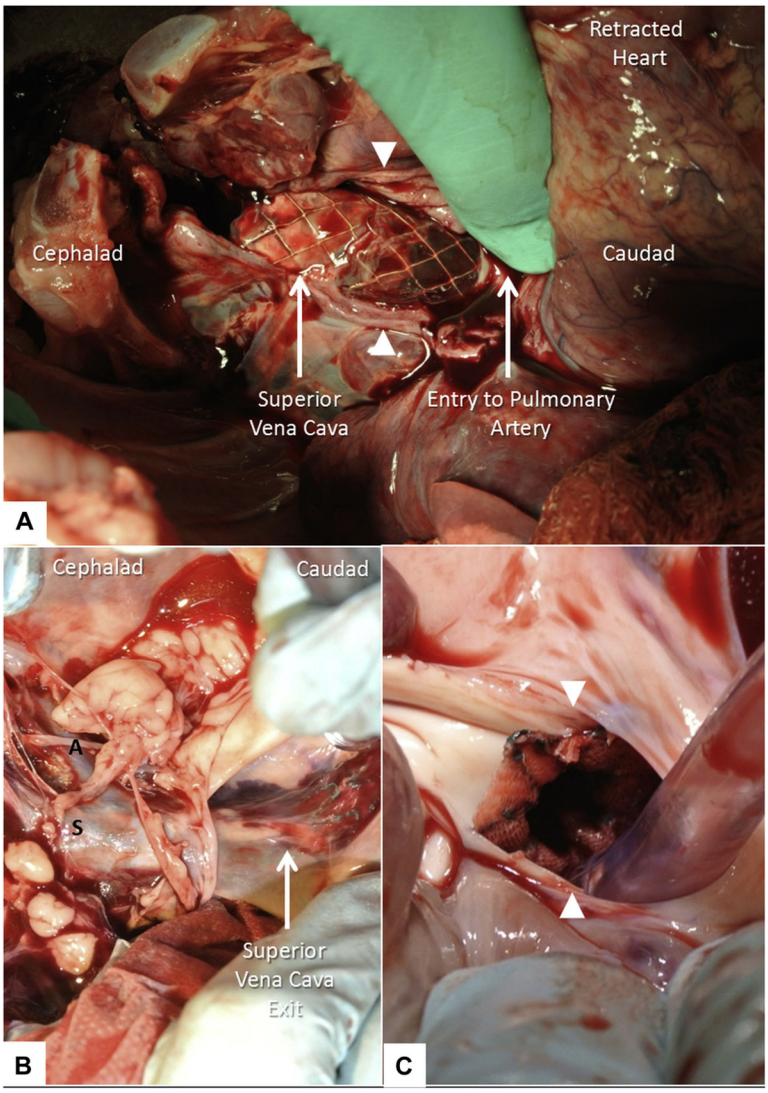

FIGURE 8. Necropsy

At necropsy, the walls of the superior vena cava **(white arrowheads)** and the rest of the heart are retracted manually to expose tandem overlapping endografts bypassing superior vena cava blood flow to pulmonary arteries **(A)**. The endograft exits the posterior wall of the superior vena cava caudad and re-enters the pulmonary artery. Similarly, the novel, purpose-built, self-expanding cavopulmonary endograft **(B, C)** bypasses superior vena cava blood flow to both branch pulmonary arteries. A = azygous vein; S = superior vena cava. The walls of the pulmonary artery **(white arrowheads)** are retracted manually **(C)** to expose distal end-to-side anastomosis of the novel endograft.

TABLE 1

Cardiac Catheterization Findings

	Baseline	Post-Intervention
Fick oximetry shunt quantification (Qp/Qs)	1.0 ± 0.1	1.0 ± 0.1
Superior vena cava diameter (mm)	14.7 ± 2.0	13.2 ± 3.0
Right pulmonary artery diameter (mm)	12.6 ± 1.7	10.5 ± 1.5 *
Left pulmonary artery diameter (mm)	11.1 ± 1.3	10.6 ± 1.6
Mean superior vena cava blood pressure (mm Hg)	1.9 ± 1.1	13.3 ± 3.0 *
Peak right pulmonary artery blood pressure (mm Hg)	14.5 ± 2.5	13.6 ± 5.2
Peak left pulmonary artery blood pressure (mm Hg)	14.5 ± 2.7	18.1 ± 4.8 *

Values are mean ± SD.

* $p < 0.05$.

TABLE 2

Magnetic Resonance Imaging Findings

	Baseline	Post-Intervention
Right ventricular end-diastolic volume (ml)	52.1 ± 15.1	49.4 ± 15.0
Right ventricular end-systolic volume (ml)	29.2 ± 12.0	31.2 ± 13.5
Right ventricular ejection fraction (%)	44.4 ± 10.3	38.1 ± 13.1*
Left ventricular end-diastolic volume (ml)	53.1 ± 6.6	41.3 ± 8.3*
Left ventricular end-systolic volume (ml)	28.1 ± 4.6	24.5 ± 6.0*
Left ventricular ejection fraction (%)	46.9 ± 6.3	41.4 ± 7.8*
Velocity-encoded MRI shunt quantification (Qp/Qs)	1.0 ± 0.2	0.9 ± 0.3
Flow: velocity-encoded MRI, aorta (ml)	20.0 ± 4.6	12.4 ± 4.1*
Flow: velocity-encoded MRI, main pulmonary artery (ml)	21.3 ± 4.9	15.3 ± 4.8*
Flow: velocity-encoded MRI, right pulmonary artery (ml)	9.3 ± 2.6	4.7 ± 2.2*
Flow: velocity-encoded MRI, left pulmonary artery (ml)	8.6 ± 3.2	6.8 ± 2.3

Values are mean ± SD.

* $p < 0.05$.

MRI = magnetic resonance imaging.